Structure-Activity Relationship Study Identifies a Novel Lipophilic Amiloride Derivative that Efficiently Kills Chemoresistant Breast Cancer Cells

Michelle Hu, Ruiwu Liu, Noemi Castro, Liliana Loza Sanchez, Julie Learn, Ruiqi Huang, Kit S. Lam, and Kermit L. Carraway, III*

Department of Biochemistry and Molecular Medicine, and

UC Davis Comprehensive Cancer Center,

UC Davis School of Medicine, Sacramento, California, USA

*Corresponding author:
Kermit L. Carraway
UC Davis School of Medicine
4645 2nd Avenue, room 1100B
Sacramento, CA 95817
Ph: 916-734-3114
Email: klcarraway@ucdavis.edu

Abstract

Derivatives of the potassium-sparing diuretic amiloride are preferentially cytotoxic toward tumor cells relative to normal cells, and have the capacity to target tumor cell populations resistant to currently employed therapeutic agents. However, a major barrier to clinical translation of the amilorides is their modest cytotoxic potency, with estimated IC_{50} values in the high micromolar range. Here we report the synthesis of ten novel amiloride derivatives and the characterization of their cytotoxic potency toward MCF7 (ER/PR-positive), SKBR3 (HER2-positive) and MDA-MB-231 (triple negative) cell line models of breast cancer. Comparisons of derivative structure with cytotoxic potency toward these cell lines underscore the importance of an intact guanidine group, and uncover a strong link between drug-induced cytotoxicity and drug lipophilicity. We demonstrate that our most potent derivative called LLC1 is preferentially cytotoxic toward mouse mammary tumor over normal epithelial organoids, acts in the single digit micromolar range on breast cancer cell line models representing all major subtypes, acts on cell lines that exhibit both transient and sustained resistance to chemotherapeutic agents, but exhibits limited anti-tumor effects in a mouse model of metastatic breast cancer. Nonetheless, our observations offer a roadmap for the future optimization of amiloride-based compounds with preferential cytotoxicity toward breast tumor cells.

35 **Introduction**

36 While amiloride has been used clinically for decades as an anti-kaliuretic in the management of
37 hypertension [1], and in the lab as a pharmacological tool for examining sodium transport [2,3],
38 substantial *in vitro* and *in vivo* data point to its anti-cancer and anti-metastatic potential [4]. High
39 concentrations of amiloride have been demonstrated to inhibit mutagen-induced carcinogenesis
40 [5-7], tumor formation [8-10] and metastatic progression [11,12] in rats and mice. These outcomes
41 are generally ascribed to the cytostatic effects of amiloride inhibition of sodium hydrogen
42 exchanger-1 (NHE1), and to the motility-suppressing effects of urokinase plasminogen activator
43 (uPA) inhibition [5].

44

45 Beyond cytostatic and anti-invasiveness activities, more recent observations indicate that
46 amiloride and its derivatives also exhibit tumor cell-selective cytotoxicity via a non-apoptotic
47 mechanism [13-16]. For example, our studies with the derivative 5-(N,N-hexamethylene)amiloride
48 (HMA) underscore the notion that the properties of amiloride derivatives may be ideally suited for
49 targeting particularly aggressive or therapy-refractory tumors [17,18]. HMA efficiently kills bulk
50 breast tumor cells independent of tumor subtype, proliferation state or species of origin, but does
51 not efficiently kill non-transformed cells derived from a variety of tissues at the same
52 concentrations. Indeed, cell lines derived from diverse tumor types are equally susceptible to
53 HMA, suggesting that its mechanism of cytotoxic action may be dependent on cellular
54 transformation rather than patient-specific genetic alterations [17,18]. Moreover, HMA is cytotoxic
55 toward breast cancer cell populations that are resistant to currently-employed therapies, including
56 the highly refractory cancer stem cell population. Finally, HMA induces morphological changes
57 within the lysosomes of tumor cells, and cytotoxicity is rescued by an inhibitor of the lysosomal
58 protease cathepsin [17,18], pointing a central role for the lysosome in its mechanism of action.

59

60 While our previous *in vitro* studies have revealed many attractive properties of amiloride
61 derivatives, and suggest that derivatization of the C(5) position of its pyrazine ring can markedly
62 enhance the tumor-selective cytotoxic properties of the drug, further translation of HMA is
63 hampered by its relatively modest potency [17,18] and poor pharmacokinetic properties in mice
64 [19]. In this study we aimed to glean further insight into structure-activity relationships (SARs)
65 within the amiloride pharmacophore by comparing the cytotoxic potential of derivatives modified
66 at the C(2) and C(5) positions. At the same time, we sought to identify more potent derivatives
67 that optimize tumor cell-specific cytotoxicity and preserve the ability to target chemoresistant
68 populations. Here we report the synthesis and characterization of 10 novel amiloride derivatives,
69 and identify a novel lead compound that acts with significantly greater potency than HMA that
70 preserves tumor-selective cytotoxicity and efficiently eradicates chemoresistant breast tumor
71 cells.

Results

Lipophilic additions to the amiloride pharmacophore increase cytotoxic potency

Amiloride is often modified at the C(2), C(5), and C(6) positions of its pyrazine ring (see Fig. 1A) to improve its transporter inhibition activity and selectivity [8,20], and such derivatives have been employed to assess the contribution of ion channel function to tumor growth and progression [4,14-19,21-29]. However, our recent studies indicating that the amiloride derivative HMA can provoke the non-apoptotic death of tumor cells relative to non-cancer cells *in vitro* by acting via the lysosome [17,18] prompt the question of whether these cytotoxic properties might be further optimized.

Figure 1

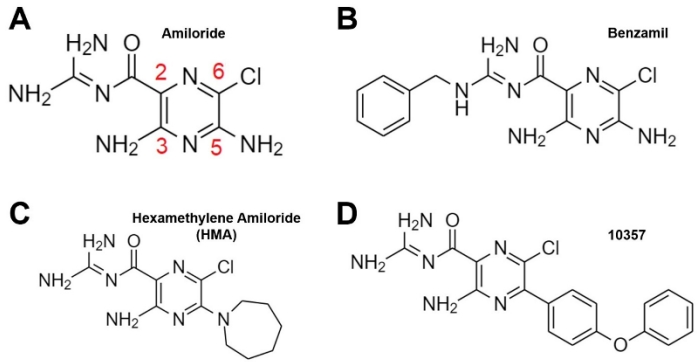

E

IC_{50} (μM)	Amiloride	Benzamil	HMA	10357
MDA-MB-231	398 ± 44	114 ± 32	36 ± 2	17 ± 2
MCF7	995 ± 341	56 ± 12	27 ± 2	15 ± 2
SKBR3	148 ± 15	50 ± 6	18 ± 1	9 ± 1

Figure 1. Modification of amiloride with lipophilic substituents enhances its cytotoxic potency. (A) Structure of amiloride with its pyrazine carbons numbered. **(B-D)** Structures of 2- and 5-substituted amiloride derivatives benzamil, HMA and 10357 are depicted. **(E)** Cytotoxic potency of amilorides toward cultured breast cancer cell lines after 24-hour treatment. Data are presented as IC_{50} (μM) averages ± SEM.

As HMA adds a lipophilic hexamethylene group to the core pharmacophore at the C(5) position, we first asked whether lipophilic modification increases the cytotoxic potency of amiloride using previously published amiloride derivatives. Fig. 1 depicts the structures of parent drug amiloride

92 (Fig. 1A), C(2) derivative benzamil (Fig. 1B), C(5) derivative HMA (Fig. 1C), and C(5) derivative
93 10357 (Fig. 1D) [26], and summarizes the cytotoxic potency of these derivatives toward cell lines
94 representing ER/PR-positive (MCF7), HER2-positive (SKBR3) and triple-negative (MDA-MB-231)
95 breast tumor subtypes in an MTT cell viability assay (Fig. 1E). Consistent with previous
96 observations [14,15,17,28,30,31], we observed that while IC_{50} values for amiloride cytotoxicity are
97 in the hundreds of micromolar, the three previously published lipophilic derivatives are 3- to 66-
98 fold more potent, and followed the general efficacy pattern 10357 > HMA > benzamil > amiloride
99 toward each of the cell line models. These observations are consistent with the notion that
100 membrane permeability and access to an intracellular target(s) may be key to the cytotoxic
101 mechanism of action.
102
103 *Novel amiloride derivatives underscore the importance of logP and the guanidine group*
104 To more rigorously test the link between amiloride derivative lipophilicity and cytotoxic potential,
105 we synthesized nine novel amiloride derivatives, most modified with various substituents at the
106 C(5) position. The structures and IC_{50} values for cytotoxicity toward the three breast cancer cell
107 line models are summarized in Table 1, and the chemical characteristics of all derivatives ordered
108 by estimated IC_{50} are summarized in Table 2. Three key points emerge from comparisons of these
109 derivatives. First, Table 2 points to a strong correlation between cytotoxic efficacy and lipophilicity,
110 reflected in partition coefficient (logP) values of the derivatives. For example, LLC1 and 10357,
111 which exhibit some of the highest logP values (2.46 and 2.88, respectively) among the group,
112 also exhibit the most potent cytotoxicity toward the breast cancer cell lines (5-13 μM and 9-17 μM,
113 respectively). On the other hand, the low logP values for amiloride and LLC10 (-0.89 and -0.28,
114 respectively) correlate with particularly poor cytotoxicity (148-995 μM and 883-2732 μM,
115 respectively). Spearman rank correlation coefficients of IC_{50} with logP were 0.0083, 0.0035, and
116 <0.0001, respectively for MDA-MB-231, MCF7 and SKBR3 cells. Second, a direct comparison of
117 derivatives LLC1 and LLC3 (Table 1) illustrates the importance of maintaining the integrity of the

118 C(2) guanidine structure. Both derivatives contain an identical lipophilic C(5) substituent, but the
119 removal of one of the guanidine amines results in a 3- to 23-fold decrease in cytotoxic potency.
120 Finally, to a first approximation each of the derivatives acts with similar potency toward all three
121 cell lines (Table 1). This suggests that, consistent with previous observations [17,18], amiloride
122 derivatives act with similar efficacy toward the different breast cancer subtypes. Overall, these
123 observations reveal new parameters for the optimization of amiloride derivatives, and highlight
124 LLC1 as a novel lead.
125

Compound	MDA-MB-231 (mM)	MCF7 (mM)	SKBR3 (mM)	Structure
LLC1	**7 ± 4**	**13 ± 2**	**5 ± 0.6**	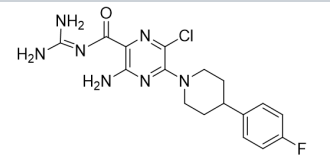
LLC2	**43 ± 5**	**54 ± 5**	**97 ± 10**	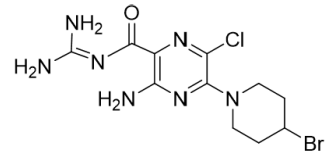
LLC3	**114 ± 25**	**75 ± 28**	**46 ± 6**	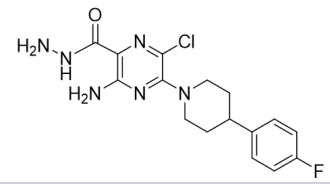
LLC4	**40 ± 5**	**56 ± 17**	**34 ± 4**	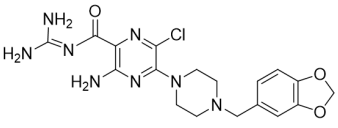
LLC5	**18 ± 1**	**29 ± 4**	**10 ± 0.6**	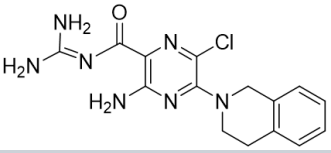

LLC7	**111 ± 41**	**138 ± 58**	**129 ± 23**	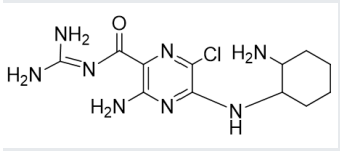
LLC8	**90 ± 11**	**75 ± 9**	**74 ± 7**	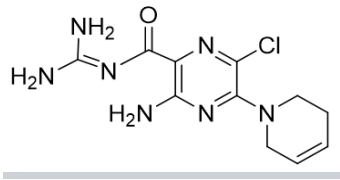
LLC9	**52 ± 7**	**55 ± 11**	**53 ± 7**	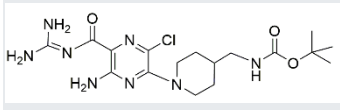
LLC10	**3000 ± 1000**	**1000 ± 3000**	**900 ± 400**	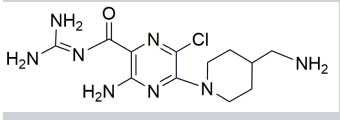

Table 1. Potencies of novel 2- & 5-substituted amiloride derivatives. Calculated IC_{50} data from MDA-MB-231, MCF7, and SKBR3 cells (24-hour treatment), and specific structures for each compound are represented in the table. Data are compiled from at least three biological replicates of each cell line and are presented as averages ± SEM.

Compound	Rule of 5	PSA ($Å^2$)	Pol ($Å^3$)	MR (cm^3/mol)	acidic pK_a	basic pK_a	pI	logP	HLB	Sol (mg/ml)	IC50 (µM)
LLC1	Y	136.5	37.3	103.4	14.8	7.1	11.0	2.5	11.5	0.015	5-13
10357	Y	142.5	39.6	102.7	14.8	5.5	10.2	2.9	11.7	0.001	9-17
LLC5	Y	136.5	33.9	94.3	14.8	7.1	11.0	1.8	12.4	0.037	10-29
HMA	Y	136.5	29.9	83.2	14.8	7.1	11.0	1.3	13.1	0.188	18-36
LLC4	N	158.2	41.7	112.8	14.8	7.1	11.0	1.2	20.0	0.060	34-56
LLC9	Y	174.8	41.1	111.5	14.5	7.1	10.8	1.2	17.7	0.121	52-55
LLC2	Y	136.5	31.0	86.2	14.8	7.1	11.0	0.9	12.7	0.152	43-97
Benzamil	Y	145.3	31.0	86.1	14.7	7.4	11.0	1.1	13.1	0.073	50-114
LLC3	Y	110.2	34.8	97.6	12.5	2.7	7.6	2.8	16.9	0.018	46-114
LLC8	Y	136.5	27.9	79.5	14.8	7.1	11.0	0.7	13.7	0.263	74-90
LLC7	Y	171.3	31.5	86.2	14.5	9.9	12.1	0.03	18.9	0.215	111-138

Amiloride	Y	159.3	19.7	56.7	14.8	7.3	11.1	-0.9	15.9	2.77	148-995
LLC10	Y	162.5	31.5	86.6	14.8	10.2	12.5	-0.3	19.2	1.10	883-2732

Table 2. Chemical and cytotoxicity characteristics of amiloride derivatives. The chemical properties of the novel amiloride derivatives are ordered according to collective cytotoxicity IC_{50} toward MCF7, SKBR3 and MDA-MB-231 breast cancer cell lines (far right column). Chemical data [Rule of 5, topological polar surface area (PSA), polarizability (Pol), molar refractivity (MR), acidic pKa, basic pKa, isoelectric point (pI), logP, hydrophilic-lipophilic balance (HLB), and intrinsic solubility (Sol)], were obtained using Chemicalize (https://chemicalize.com, developed by ChemAxon).

LLC1 preferentially reduces the viability of murine mammary tumor organoids ex vivo

We have previously demonstrated that HMA reduces the viability of organoids derived from the PymT and NDL genetically-engineered mouse models of breast cancer [18]. To determine whether LLC1 is selectively cytotoxic toward mammary tumors relative to normal tissue, we compared its impact on tumor and normal mammary gland organoids generated from Balb/cJ mice orthotopically engrafted with 4T1 ($ER^-/PR^-/HER2^-$), an isogenic murine mammary cancer cell line. The approximate IC_{50} value of LLC1 toward human tumor cell lines (10 μM, Table 1) was used to compare the efficiency of cell death as a function of time. We observed that while LLC1 reduces the viability of tumor organoids over 72 hours of treatment (Figs. 2A and 2B), normal mammary gland organoids tend to be resistant to LLC1 treatment (Figs. 2C and 2D). These observations suggest that, similar to its predecessor HMA [17,18], LLC1 exhibits significant selectivity toward cancer cells and leaves untransformed cells largely unharmed.

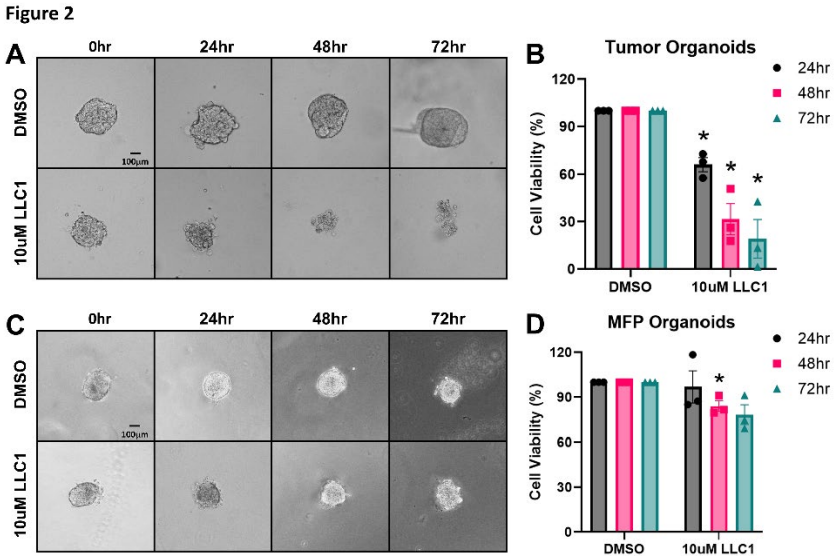

Figure 2. LLC1 selectively reduces the viability of mouse mammary tumors *ex vivo*. Representative images of LLC1-treated (10 µM) organoids generated from mammary tumors **(A)** and normal mammary glands **(C)** from 4T1-engrafted Balb/cJ mice are shown. Scale bar = 100 µm. **(B, D)** Organoids were treated with 10 µM LLC1, and viability was assessed using RealTime Glo over 72 hours and normalized to vehicle treatment (DMSO). Tumor **(B)** or mammary fat pad (MFP) **(D)** organoid viability was monitored every 24 hours. Data were compiled from three biological replicates of organoids derived from tumors or mammary glands of independent mice. Data are presented as averages ± SEM and significance assessed by t-test. *, $P < 0.05$.

LLC1 acts on chemoresistant breast cancer cell populations

Our previous observations indicate that HMA is cytotoxic toward 'persister' populations of breast cancer cells that survive 3-9 day exposure to conventional chemotherapeutic agents cisplatin, docetaxel and doxorubicin (DOXO) [18]. To confirm HMA's capabilities and test LLC1's properties, we examined the impact of both drugs on the viability of various breast cancer cell line models of short-term and established therapeutic resistance. We first examined the response of chemoresistant populations of MDA-MB-231 cells toward the derivatives. In the experiment shown in Fig. 3, cells were first pretreated for 48 hours with DMSO vehicle, and then further treated for 24 hours with DMSO, 250 nM docetaxel (DTX), 5 µM DOXO, and either 40 µM HMA (Fig. 3A) or 10 µM LLC1 (Fig. 3D). In each case, drug treatment lowered cell viability by 15-40%, confirming that the drugs behave as expected. However, in cells pretreated for 48 hours with either DTX (Figs. 3B and 3E) or DOXO (Figs. 3C and 3F), a second challenge with the pretreating

drug did not reduce viability while HMA or LLC1 treatment lowered viability by 25-60%, consistent with the interpretation that chemotherapy-resistant populations are sensitive to amiloride derivatives.

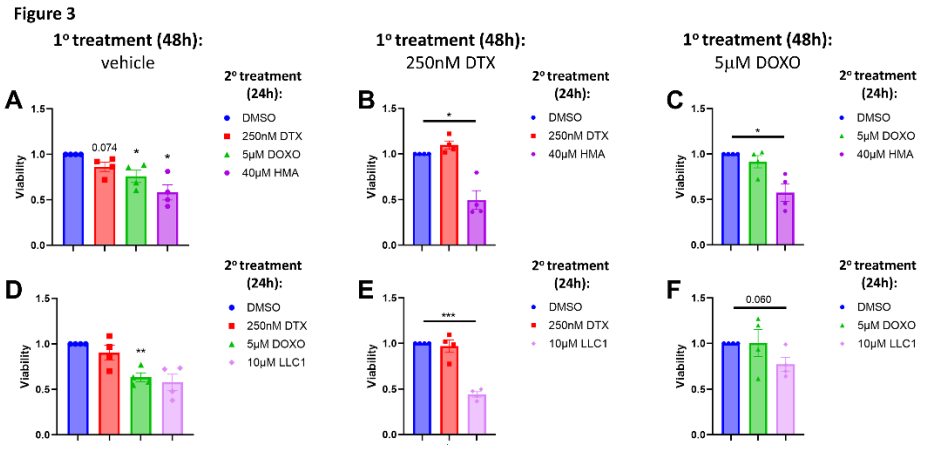

Figure 3. HMA and LLC1 are cytotoxic toward chemoresistant triple-negative breast cancer cell populations. (A,D) MDA-MB-231 cells were initially treated with vehicle (DMSO) for 48 hours, followed by a second challenge with DMSO, 250 nM docetaxel (DTX), 5 μM doxorubicin (DOXO), or either 40 μM HMA **(A)** or 10 μM LLC1 **(D)** for 24 hours, and then cell viability was determined by MTT assay. **(B,C,E,F)** Following 48 hours 250 nM DTX **(B,E)** or 5 μM DOXO **(C,F)** pretreatment, residual cells were treated with vehicle, initial chemotherapy treatment (DTX or DOXO), HMA **(B,C)**, or LLC1 **(E,F)** for an additional 24 hours. Data represent a minimum of four biological replicates and are presented as averages ± SEM, and significance was assessed by t-test. *, $P < 0.05$; **, $P < 0.01$; ***, $P < 0.001$.

We further observed that roughly half of T47D cells, an ER/PR$^+$ breast cancer cell line, exhibit resistance to cell death induced by 72-hour treatment with doxorubicin (DOXO, Fig. 4A) and docetaxel (Fig. 4D), reflected in the inability of high doses of either drug to further impact viability in a titration. However, we found that both HMA and LLC1 are cytotoxic toward the residual population that remains after chemotherapeutic treatment (Figs. 4B, 4C and 4E, 4F), and exhibit similar IC_{50} values as cell lines representing a variety of solid tumor types (Table 1).

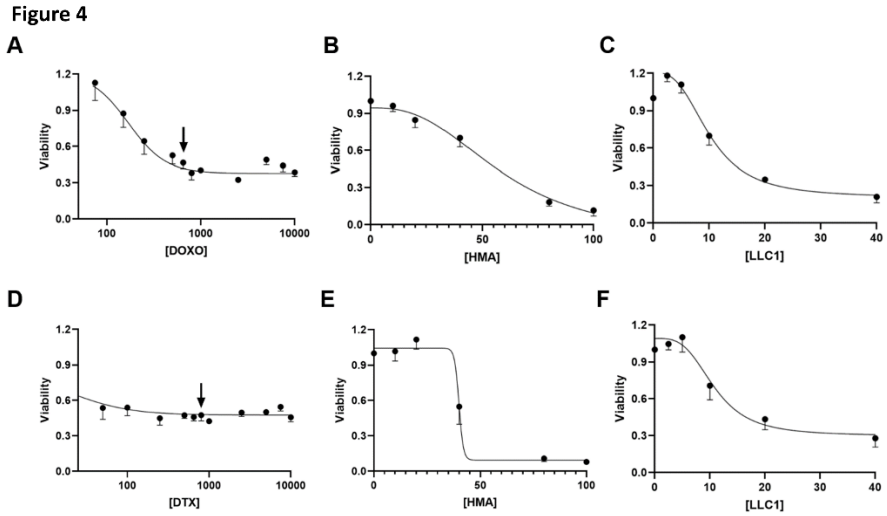

Figure 4. HMA and LLC1 are cytotoxic toward chemoresistant ER/PR-positive breast cancer cell populations. Dose-response curves of T47D cells treated with doxorubicin (DOXO) **(A)** or docetaxel (DTX) **(D)** for 72 hours are depicted. Populations of cells that persist at drug concentrations higher than 650 nM DOXO and 800 nM DTX (arrows) are considered drug resistant. Residual T47D cells that survive treatment with these levels of drugs for 72 hours were then titrated with HMA **(B,E)** or LLC1 **(C,F)** for an additional 24 hours and viability assessed. Data are compiled from at least three biological replicates.

Additionally, we observed that a breast cancer cell line selected for stable therapeutic resistance is as sensitive to amiloride derivatives as the drug-sensitive parental line. MX-100 [32] is a derivative of MCF7 cells selected for stable mitoxantrone resistance that overexpresses ABCG2 (aka breast cancer resistance pump, BCRP) by 30-fold. MCF7 TR-1 and MCF7 TR-5 [33] are stable tamoxifen resistant derivatives, while MCF TS is (z)-4-hydroxytamoxifen (TAM) sensitive. Each cell line was treated with varying concentrations of TAM, DTX, DOXO, HMA, and LLC1, and cytotoxicity IC_{50} values were determined (Table 3). We observed that parental MCF7 cells are 3-13 fold more sensitive to chemotherapeutic agents DTX and DOXO than MX-100, but both cell lines are similarly sensitive to HMA and LLC1. Likewise, MCF7 TS cells are far more sensitive to tamoxifen than MCF7 TR-1 and MCF7 TR-5 cells, but all three lines are similarly sensitive to HMA and LLC1. Collectively, these observations provide strong evidence that amiloride derivatives act on breast tumor cell populations that are resistant to clinically pertinent anti-cancer agents.

Cell Line	TAM (mM)	DTX (mM)	DOXO (mM)	HMA (mM)	LLC1 (mM)
MCF7	-	1 ± 0.6	2 ± 0.3	27 ± 2	13 ± 2
MCF7 MX-100	-	13 ± 3	7 ± 0.5	39 ± 3	12 ± 1
MCF7 TS	13 ± 1	-	-	68 ± 3	25 ± 1
MCF7 TR-1	ND	-	-	67 ± 4	26 ± 2
MCF7 TR-5	ND	-	-	59 ± 5	19 ± 2

218 **Table 3.** MCF7 chemoresistant cells are susceptible to amiloride derivatives but not conventional
219 chemotherapeutics. The table depicts parent and chemoresistant MCF7 cell line derivatives
220 titrated with chemotherapeutic agents tamoxifen (TAM), docetaxel (DTX), doxorubicin (DOXO),
221 HMA, or LLC1 for 24 hours to determine their IC_{50} values. ND denotes that an IC_{50} value could
222 not be determined due to the very high dosage required. Data represent a minimum of three
223 independent biological replicates and are presented as averages ± SEM.
224

225 Finally, we observed that both HMA and LLC1 are as cytotoxic toward diverse mammalian cell
226 line models of cancer as human breast cancer cell line models. In the experiments summarized
227 in Supplementary Table S3, we assessed the cytotoxic potencies of HMA and LLC1 toward Met-
228 1 (triple-negative), NDL (HER2-positive), and 4T1 (triple-negative) murine breast cancer cells, as
229 well as UCDK9MM3 (melanoma), UCDK9OSA29 (osteosarcoma), and D17 (osteosarcoma)
230 canine tumor cell lines. We observed that HMA provokes the death of all models with IC_{50} values
231 in the 20-40 μM range, while LLC1 induces cytotoxicity in the 7-14 μM range. These values are
232 consistent with their potencies toward human breast cancer cell lines (Table 1), collectively
233 providing support for the notion that amiloride derivatives act to eradicate transformed cells in a
234 tumor type-, subtype-, and species-agnostic manner.
235

236 *LLC1 provokes little observable tissue toxicity or anti-tumor effects* in vivo

As a more potent cytotoxic agent than HMA, we sought to assess the *in vivo* anti-tumor efficacy of LLC1 using the orthotopic, immune-intact 4T1-Balb/c model of metastatic triple-negative breast cancer. We began by performing a maximum tolerated dose (MTD) study with Balb/cJ mice, where animals were intraperitoneally injected with 0 mg/kg, 15 mg/kg, 30 mg/kg, and 45 mg/kg LLC1 three times over the course of one week. In this experiment we observed no obvious fluctuations in body weight (Fig. 5A) or aberrant behaviors in any of the animals. Likewise, bloodwork revealed no significant changes at any LLC1 treatment level in markers of liver and kidney damage compared to control (0 mg/kg LLC1) or the reference values (Fig. 5B). Moreover, organs including spleen, heart, liver, and kidneys exhibited no gross morphological (Figs. 5C-F) or histopathological differences (Supplementary Fig. S15) with LLC1, suggesting that under the employed treatment conditions LLC1 is well tolerated by mice.

Figure 5

A

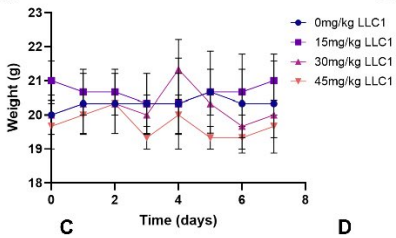

B

Dose (mg/kg)	ALT (U/L)	AST (U/L)	Albumin (g/dL)	Alk Phos (U/L)	BUN (mg/dL)	Creatinine (mg/dL)	Total Bilirubin (mg/dL)	Total Protein (g/dL)
0	83 ± 13	240 ± 46	3.1 ± 1.0	121 ± 41	13.6 ± 3.1	0.12 ± 0.01	0.037 ± 0.023	4.3 ± 1.5
15	312 ± 270	484 ± 354	2.7 ± 1.2	106 ± 47	12.1 ± 3.7	0.12 ± 0.02	0.082 ± 0.058	3.7 ± 1.6
30	81 ± 23	226 ± 86	3.9 ± 0.1	152 ± 6	14.5 ± 1.8	0.14 ± 0.01	0.039 ± 0.006	5.2 ± 0.04
45	111 ± 19	271 ± 44	2.9 ± 1.3	158 ± 72	14.9 ± 5.9	0.15 ± 0.04	0.062 ± 0.011	3.8 ± 1.7
Ref	0 - 403	0 - 552	2.9 – 4.0	49-172	15.2 – 34.7	0.0 - 0.3	0.0 – 0.2	4.7 – 6.1

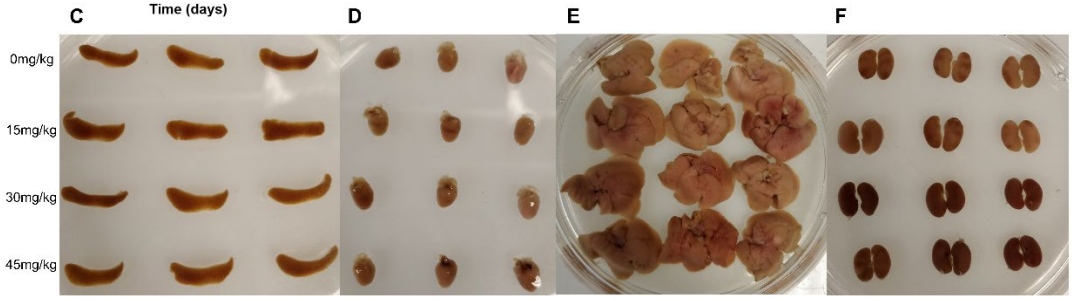

Figure 5. LLC1 is well tolerated by mice. Adult Balb/cJ mice were injected intraperitoneally with 0-45 mg/kg LLC1 on days 0, 3 and 6 of the study and sacrificed on day 7. **(A)** Body weights were recorded throughout the study. **(B)** A blood chemistry panel illustrates the effects of repeated LLC1 treatment on liver (ALT, alanine transaminase; AST, aspartate transaminase; albumin; alk phos, alkaline phosphatase; total bilirubin; total protein) and kidney (BUN, blood urea nitrogen; creatinine; total protein) markers. Images of mouse **(C)** spleen, **(D)** heart, **(E)** liver, and **(F)** kidneys are displayed for each dose after formalin fixation.

To assess the impact of LLC1 on tumor growth properties we orthotopically implanted 4T1 cells into the mammary fat pads of Balb/cJ mice. A treatment paradigm of intraperitoneally-delivered vehicle or 30mg/kg LLC1 three times per week for three weeks was initiated after tumors reached 100mm^3 in volume (Fig. 6A), and animals were sacrificed a day after the last dose. Tumor volume (Fig. 6B) and mouse body weight (Supplementary Fig. S16) were monitored over the course of treatment, and tumor volume (Fig. 6C), number of metastatic lesions observed per lung lobe (Fig. 6D), and the area of metastatic coverage (Fig. 6E), were recorded at the experimental endpoint. We observed no statistically significant differences in tumor growth and metastatic characteristics upon treatment of animals with LLC1. Importantly, inspection of primary tumors revealed no evidence of increased necrotic cell death with LLC1 treatment, strongly suggesting that drug dosing or delivery was insufficient to impact tumor characteristics.

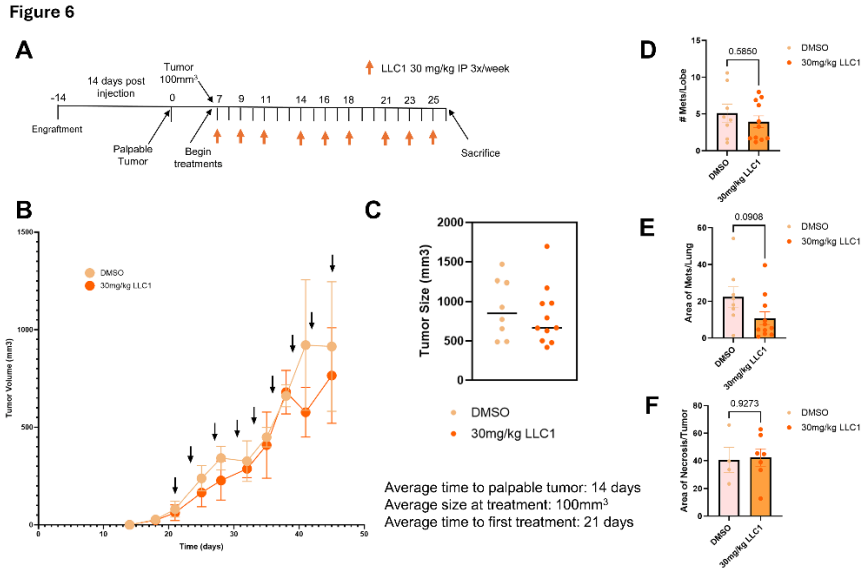

Figure 6. LLC1 exhibits limited therapeutic efficacy toward a 4T1-Balb/cJ model of metastatic breast cancer. (A) Schematic of the treatment regimen is illustrated, where animals are treated three times per week for three weeks with vehicle (n=8) or 30mg/kg LLC1 (n=11) after tumors reach 100mm^3 in volume, and sacrificed 19 days after the initial injection. **(B)** Tumor volumes were determined for animals treated with vehicle and LLC1. Averages ± SEM at each time point are depicted. **(C)** Tumor volumes at sacrifice are compared. Metastatic burden was established through analysis of metastatic lesions per lobe **(D)** and metastatic area of the lung **(E)**. **(F)** Area of necrosis was evaluated between vehicle- and LLC1-treated cohorts. Differences in metastatic burden parameters and necrotic area were compared by t-test.

280 **Discussion**

281 Amiloride derivatives offer significant promise as anticancer therapeutic agents because they
282 exhibit tumor cell-selective cytotoxicity and harbor the potential to eradicate chemoresistant tumor
283 cell populations [18]. However, modest potency and poor pharmacokinetic properties have
284 hampered efforts to translate these agents. The optimization of amiloride structure is an enticing
285 area for medicinal chemists and biologists alike because the relative ease of synthesis and
286 chemical modification allow the straightforward development of new derivatives while optimizing
287 its unique anticancer properties. Our study reveals that LLC1, a novel lipophilic C(5) amiloride
288 derivative, induces cell death in the single digit micromolar range, selectively kills tumor organoids
289 relative to normal mammary gland organoids, and eradicates chemoresistant breast cancer cell
290 populations. Collectively, our observations demonstrate that systematic analysis of amiloride
291 pharmacophore modification can lead to improved anticancer drug candidates, agents that have
292 the capacity to act across many tumor types, subtypes and even species.

293

294 Importantly, our SAR analysis provides two key insights into building more effective cancer-
295 selective cytotoxic amiloride derivatives. First, we observed a strong relationship between
296 amiloride lipophilicity, reflected in more positive logP values, and drug cytotoxicity. Indeed, our
297 most potent derivative LLC1 exhibits one of the highest logP values of the compounds we have
298 examined, suggesting that further increases in lipophilicity could result in even more effective drug
299 leads. These conclusions dovetail with current trends in drug development that prioritize more
300 lipophilic drugs because of their higher likelihood of passing safety and ADME concerns during
301 Phase 1 clinical studies [34]. Second, disruption of the guanidine moiety at the C(2) position
302 appears deleterious to cytotoxic function. LLC1 and LLC3 are identical except for the deletion of
303 one of the guanidine amino groups in LLC3, and this change leads to an order of magnitude loss
304 of potency. In this regard it might be interesting to determine whether lipophilic derivatives of other

305 existing guanidine-containing drugs, or lipophilic compounds containing multiple guanidine
306 groups, might similarly exhibit tumor cell-selective cytotoxicity and improved efficacy.
307
308 Our findings strongly suggest that amilorides act as cationic amphiphilic drugs (CADs), a broad
309 class of agents defined by the presence of both a lipophilic moiety and a hydrophilic ionizable
310 amine [16,35,36]. Over five dozen FDA-approved agents fit the general structural definition of
311 CADs, including antidepressants, antibiotics, antiarrhythmics, and diuretics [16,36]. CADs
312 characteristically accumulate in lysosomes and frequently provoke lysosome-mediated lipidosis
313 which can be followed by cell death, and for this reason investigators will often disregard hits with
314 these agents in drug screens [35]. However, the tumor-selective cytotoxicity of this drug class,
315 together with observations that lipidotic responses may be readily reversed upon CAD withdrawal
316 [35,36], underscore the existence of a therapeutic window that might be exploited for cancer
317 patient benefit.
318
319 Their high degree of hydrophobicity allows CADs to spontaneously cross membranes, while the
320 low pH of the lysosome facilitates drug protonation, luminal trapping and accumulation, and
321 disruption of lysosomal hydrolase activities. Enzymes of the lysosomal sphingolipid catabolic
322 cascade appear particularly susceptible to CADs, possibly because electrostatic interactions of
323 these enzymes and their chaperones with highly acidic intraluminal vesicles required for enzyme
324 function are shielded by the positively charged agents [35,36]. The resulting accumulation of
325 sphingolipid substrates then destabilizes the lysosomal limiting membrane, leading to lysosomal
326 membrane permeabilization (LMP) and lysosome-dependent cell death (LDCD) [37-40]. A variety
327 of cellular stressors, including cationic amphiphilic drugs, microtubule inhibitors, nanoparticles
328 and lysosomotropic detergents, can damage and permeabilize the limiting lysosomal membrane.
329 Beyond compromising lysosome function, LMP leads to the release of lysosomal hydrolases that
330 act on cytosolic substrates to elicit a cascade of events culminating in cytolysis, the defining event

in necrotic cell death [40]. Importantly, sequestration of CADs at the site of their targets in the lysosome and shielded from drug resistance-mediating plasma membrane drug pumps whose expression is common to many chemoresistant tumor cells may contribute to the sensitivity of chemoresistant cells to amiloride derivatives.

Two features of LMP/LDCD make the engagement of this cell death mode particularly attractive for anti-cancer therapeutics development. First, lysosomal membranes of transformed cells are inherently more fragile than those of normal cells [38,41], explaining tumor cell selectivity of amiloride derivatives and offering a potential therapeutic window that might be exploited clinically. Second, we have observed both previously and in this study that chemoresistant cells, including cancer stem cells (CSCs), are as susceptible to this form of cell death as are differentiated (bulk) cancer cells [40]. CSCs are the rare subpopulation of tumor cells responsible for both tumor recurrence and metastasis, are notoriously resistant to chemotherapeutic and targeted therapeutic agents [42,43], and remain a vexing barrier to achieving substantially improved patient outcomes. The similar susceptibility of CSCs and bulk cancer cells to LMP/LDCD suggests that CSC subpopulations cannot easily escape LMP/LDCD-inducing therapeutic agents to initiate primary or metastatic recurrence through reversion to the differentiated state. This then raises the possibility that these agents could be significantly more effective in altering patient outcomes than existing anti-cancer drug classes.

The limited anti-tumor effects of LLC1 *in vivo* is disappointing but not surprising. Previous studies demonstrate that HMA has a very short half-life in mice [19], and in our previous studies we were only able to observe significant anti-tumor effects of HMA when we encapsulated the drug in a disulfide-linked nanoparticle that markedly prolongs half-life [18]. Since we strongly suspect that drug elimination is a central issue with LLC1, future studies will be aimed at identifying higher potency amiloride derivatives with more favorable pharmacokinetic properties.

357 **Materials and Methods**

358 *Cell Culture and Drug Treatments*

359 Human breast cancer cell lines MDA-MB-231, MCF7, SKBR3, and T47D, and mouse mammary
360 cancer cell line 4T1, were purchased from American Type Culture Collection (Manassas, VA,
361 USA) and maintained at 37°C and 10% CO_2 in Dulbecco's Modified Eagle Medium (DMEM)
362 supplemented with 10% fetal bovine serum (Genesee Scientific) and antibiotics
363 (penicillin/streptomycin; Gibco - Thermo Fisher). MCF7-B7-TS (MCF7 TS), MCF7-G11-TR-1
364 (MCF7 TR-1), MCF7-G11-TR-5 (MCF7 TR-5), and MCF7 MX-100 cells were obtained from the
365 Physical Sciences-Oncology Network Bioresource Core Facility at ATCC or gifted from Dr. A.M.
366 Yu, UC Davis. The tamoxifen (TAM) resistant lines were maintained in MCF7 base media
367 supplemented with 1 μM or 5 μM TAM [44]. The mitoxantrone resistant line (MX-100) was
368 maintained as previously described [45]. Met-1 (gifted by A.D. Borowsky, UC Davis) and NDL
369 murine cells were maintained as previously described [46,47]. UCDK9MM3, UCDK9OSA27, and
370 D17 canine cells (gifted by R.B. Rebhun, UC Davis) were maintained as previously described [48-
371 50]. Cell line attributes are summarized in Supplementary Table S1.

372

373 Amiloride, HMA, benzamylamiloride (benzamil), and amiloride derivative 10357 were sourced as
374 described in Supplementary Table S2, applied to cells at 50-70% confluency in DMSO (final
375 vehicle concentration <0.5%), and analysis of amiloride derivative cytotoxicity was carried out
376 after 24 hours except in the case of the organoid experiment (up to 72 hours). In some
377 experiments cells were titrated (Fig. 4) with chemotherapeutic agents (docetaxel, 0-10μM;
378 doxorubicin, 0-10μM), or were pretreated with agents (docetaxel, 0.65 μM; doxorubicin, 0.8 μM)
379 to pre-select for short-term drug resistance prior to treatment with amiloride derivatives (Fig. 3).

380

381 *Design and Synthesis of Novel Amiloride Derivatives*

382 The new amiloride derivatives were designed to introduce novel hydrophobic groups at the C(5)
383 position to improve cell permeability and potential *in vivo* availability. Synthesis of LLC1 was
384 carried out as shown in Supplementary Fig. S1. To a suspension of methyl 3-amino-5,6-dichloro-
385 2-pyrazinecarboxylate (compound **1**; 444 mg, 2.0 mmol) in anhydrous dimethylformamide (DMF;
386 3 mL) was added 4-(4-fluorophenyl)piperidine (compound **2**; 358.5 mg, 2.0 mmol) and *N*,*N*-
387 Diisopropylethylamine (697 μL, 4.0 mmol), the reaction mixture was stirred at room temperature
388 overnight and then added to cold water. The precipitate was collected by centrifuge and washed
389 with water. The crude product (compound **3**) was used for the next step without further purification.
390 0.5 M $NaOCH_3$ solution in CH_3OH (20 mL) was added to guanidine hydrochloride (955.3 mg, 10
391 mmol) and the resulting mixture was stirred at room temperature for 0.5 hr. The white precipitate
392 was removed by filtration, and the free guanidine solution in methanol was added to a suspension
393 of methyl ester (compound 3; 364.8mg, 1.0 mmol) in DMF (5 mL) and stirred at room temperature
394 overnight. Brine (20 mL) was added, and the mixture extracted with ethyl acetate (3 × 30 mL).
395 The organic layer was washed with 10% NaCl (2 × 30 mL), dried over anhydrous Na_2SO_4, and
396 concentrated under reduced pressure. The crude mixture was dissolved in 5 mL of 30%
397 CH_3CN/70% H_2O and 0.1% trifluoroacetic acid and purified by a reverse phase HPLC. The
398 collected eluent was lyophilized to yield the designed product LLC1. The structure was verified by
399 Orbitrap high resolution ESI-MS: calculated 392.1402, found 392.1391 [M+1] (Supplementary Fig.
400 S2A). The purity was >98% as shown in HPLC (Supplementary Fig. S2B). LLC3 was synthesized
401 by mixing compound **3** in DMF with 1.0 M hydrazine (10 eq.) in ethanol overnight (Supplementary
402 Fig. S1). The chemical identity and purity were verified by ESI-MS and HPLC (Supplementary
403 Figs. S3A and 3B), respectively.
404
405 Other LLC compounds were synthesized using a similar approach with modification. Different
406 amines were used to displace the C5-Cl in compound **1**: 4-bromopiperidine hydrobromide (**4**) for
407 LLC2 and LLC8, -piperonylpiperazine (**6**) for LLC4, 1,2,3,4-tetrahydroisoquinoline (**7**) for LLC5,

408 1,2-diaminocyclohexane (**8**), tert-butyl methyl(piperidin-4-ylmethyl)-carbamate (**12**) for LLC9 and
409 LLC10. The synthetic approach of LLC2 and LLC8 is shown in Fig. S4. LLC4, LLC5 and LLC7
410 were prepared as shown in Fig. S5. The synthesis of LLC9 and LLC10 is shown in Fig. S6.
411 Treatment of LLC9 with 50% trifluoroacetic acid in dichloromethane (DCM) for 1 hour yielded
412 LLC10. All LLC compounds have purity >95% as shown in HPLC and their identities were verified
413 by HR ESI-MS (Figs. S7-S13).
414
415 *MTT Assay*
416 Cells were seeded on 24-well plates and cultured to 50-70% confluency prior to treatment with
417 various compounds for 24-72 hour depending on the assay context. Following treatments, media
418 was aspirated from cells and replaced with 5 mg/mL 3-(4,5-Dimethyl-2-thiazolyl)-2,5-diphenyl-2H-
419 tetrazolium bromide (MTT, #M5655, Sigma Aldrich) solution in base media. Cells were incubated
420 at 37°C for 1-2 hours to induce formazan crystal formation, then washed with phosphate-buffered
421 saline (PBS) to remove impurities. Crystals were dissolved using isopropyl alcohol (0.5% 1N HCl
422 in isopropanol), and sample absorbance (λ_{ex} 570 nm) was measured with a FilterMax F5
423 microplate reader (Molecular Devices) and Multi-Mode Analysis software (Version 3.4.0.27,
424 Beckman Coulter). The reported IC_{50} values for each drug were calculated from the concentration
425 required to induce half-maximal suppression of absorbance across 3-4 biological replicates.
426
427 *Ex Vivo Drug Cytotoxicity Organoid Assay*
428 Tumors were harvested after 1 x 10^6 4T1 cells engrafted into Balb/cJ mice (#000651, The Jackson
429 Laboratory) at the 4th mammary fat pad were grown to 1.0-1.5 cm in diameter. Tumors or pooled
430 mammary glands from Balb/cJ mice were chopped into fine pieces using a razor blade before
431 addition to digestion buffer (DMEM/F12 #SH30023, HyClone;1% PenStrep, Gibco - Thermo
432 Fisher; 2% fetal bovine serum (FBS), Genesee Scientific; collagenase/hyaluronidase (5%: tumors
433 & 10%: mammary glands), #07912, StemCell Technologies; 5 mg/mL insulin, Gibco - Thermo

434 Fisher) and vortexed. Samples were digested for 2hr at 37°C with gentle shaking, and samples
435 vortexed every 30 minutes, before they were processed. After neutralization of the digestion buffer
436 with DMEM (Gibco - Thermo Fisher) containing 10% FBS, organoids were centrifuged at 700 rpm
437 to remove cellular debris. ACK lysis buffer (Gibco - Thermo Fisher) was used to remove red blood
438 cells from the organoids. A quick spin was performed to remove additional debris and to pellet
439 organoids. Once resuspended in PBS, organoids were embedded into MatriGel (#354230,
440 Corning) and cultured in organoid growth media (OGM) on 24-well plates for 24 hours as
441 described previously [51]. After overnight incubation in OGM, organoids were treated with vehicle
442 or 10 μM LLC1 for up to 72 hours, and viability was measured using RealTime Glo (#G9711,
443 Promega) according to manufacturer's instructions. Images were taken before drug treatment (0
444 hour) and every 24 hour over the course of drug treatment. Representative brightfield images
445 were taken with an Olympus IX81 microscope with CellSens Entry software. Chemiluminescent
446 images were taken with a ChemiDoc Touch Imaging System (BioRad) and analyzed with FIJI
447 (https://imagej.net/Fiji) software to quantify RealTime Glo signal.
448
449 *Statistical, Data, and Image Analysis*
450 A minimum of three biological replicates per experiment was performed with values calculated
451 and expressed as averages ± standard error of the mean (SEM), unless otherwise stated.
452 Statistical significance was between control and test arms was determined using paired t-test; P-
453 values of less than 0.05 were considered statistically significant. Data analysis was performed
454 using Microsoft Excel or GraphPad Prism version 9.3.1 for Windows (GraphPad Software; San
455 Diego, CA, USA; www.graphpad.com). Images were compiled in Microsoft PowerPoint and only
456 brightness and contrast were altered for clarity.
457
458 *Maximum Tolerated Dose Study*

459 All animal studies were performed in accordance with protocols approved by the Institutional
460 Animal Care and Use Committee (IACUC) of the University of California, Davis. 8-10 week old
461 Balb/cJ mice (000651) were purchased from The Jackson Laboratory and were acclimated to the
462 animal room for at least one week prior to use. To determine the maximum tolerated dose (MTD)
463 for LLC1, mice (n=3/cohort) were randomly separated into four groups and injected
464 intraperitoneally with 0mg/kg (10% DMSO in saline), 15mg/kg, 30mg/kg, and 45mg/kg LLC1 in
465 10% DMSO in saline three times over seven days. Body weights and clinical signs were observed
466 daily. Mice were sacrificed the day following the third treatment after cardiac puncture to collect
467 blood. After coagulation and separation by centrifugation, serum was collected for blood chemistry
468 panel analysis. Organs were harvested and fixed in 10% neutral buffered formalin for paraffin
469 embedding and sectioning.
470
471 *LLC1 Therapeutic Efficacy Study*
472 $2x10^5$ 4T1 cells in PBS were mixed in a 1:1 volume/volume ratio with PuraMatrix Peptide Hydrogel
473 (#354250, Corning) and injected bilaterally into the 4th mammary fat pads of 8-10 week old Balb/cJ
474 mice under anesthesia by continuous inhalation of 2% isoflurane gas. The 4th nipple was used as
475 a landmark for injection into the mammary gland with sterile tweezers lifting the nipple while the
476 syringe needle loaded the cell suspension into the mammary fat pad. Tumor dimensions were
477 measured twice per week with digital calipers and tumor volume calculated according to the
478 formula $v = (w^2 \times l) \times 0.5236$. Once tumors reached $100mm^3$, animals were randomized into two
479 cohorts: 8 mice injected with 10% DMSO in saline and 11 mice injected with 30g/kg LLC1 in 10%
480 DMSO in saline. Mice were injected intraperitoneally with their appropriate dose three times per
481 week for three weeks before sacrifice by CO_2 asphyxiation the day after the last treatment.
482 Tumors and organs were harvested and fixed in 10% neutral buffered formalin for paraffin
483 embedding and sectioning.
484

485 *Histology*

486 H&E-stained sections of tumors, liver, kidney and heart were prepared as previously described
487 [52]. 5μm sections were imaged using Keyence microscope BZ-X800, and LLC1 toxicity was
488 assessed based on any morphologic changes. For the therapeutic study, all xenograft tumors
489 were subjected to histological analysis. For tumors, the area of active necrosis was quantified and
490 normalized to total tumor area from 2-6 randomly selected fields across three serial sections.
491 Staining of lungs for metastatic lesions was modified from whole mount mammary gland and
492 tumor protocols previously described [52]. Briefly, lungs were dehydrated, cleared, and stained
493 with Mayer's hematoxylin before imaging of macrometastases with a dissecting scope (Zeiss
494 Stemi 2000-C; Axiocam ERc/5s). Analyses of lesions were performed using two approaches: 1)
495 lesions were counted per lung lobe and averaged between two different slides, and 2) lesion area
496 was quantified and averaged between total lung area. Lungs were then rehydrated and processed
497 to confirm histology.

498 **References**

499 1. Sun, Q. & Sever, P. Amiloride: A review. *J Renin Angiotensin Aldosterone Syst* **21**,
500 1470320320975893; 10.1177/1470320320975893 (2020).
501
502 2. Horisberger, J. D. Amiloride-Sensitive Na Channels. *Current Opinion in Cell Biology*
503 **10**, 443-449 (1998).
504
505 3. Kleyman, T. R. & Cragoe, E. J., Jr. Cation transport probes: the amiloride series.
506 *Methods Enzymol* **191**, 739-755 (1990).
507
508 4. Matthews, H. M., Ranson, M. & Kelso, M. J. Anti-tumour/metastasis effects of the
509 potassium-sparing diuretic amiloride: an orally active anti-cancer drug waiting for its
510 call-of-duty? *Int J Cancer* **129**, 2051-2061 (2011).
511
512 5. Tatsuta, M. *et al*. Inhibition by amiloride of gastric carcinogenesis induced by N-
513 methyl-N'-nitro-N-nitrosoguanidine in Wistar rats. *Br J Cancer* **67**, 1011-1014 (1993).
514
515 6. Tatsuta, M. *et al*. Inhibition by amiloride of experimental carcinogenesis induced by
516 azaserine in rat pancreas. *Cancer Lett* **106**, 23-28 (1996).
517
518 7. Tatsuta, M. *et al*. Chemoprevention by amiloride against experimental
519 hepatocarcinogenesis induced by N-nitrosomorpholine in Sprague-Dawley rats.
520 *Cancer Lett* **119**, 109-113 (1997).
521
522 8. Kleyman, T. R. & Cragoe, E. J., Jr. Amiloride and its analogs as tools in the study of
523 ion transport. *J Membr Biol* **105**, 1-21 (1988).
524
525 9. Sparks, R. L., Pool, T. B., Smith, N. K. & Cameron, I. L. Effects of amiloride on tumor
526 growth and intracellular element content of tumor cells in vivo. *Cancer Res* **43**, 73-77
527 (1983).
528
529 10. Jankun, J., Keck, R. W., Skrzypczak-Jankun, E. & Swiercz, R. Inhibitors of urokinase
530 reduce size of prostate cancer xenografts in severe combined immunodeficient
531 mice. *Cancer Res* **57**, 559-563 (1997).
532
533 11. Kellen, J. A., Mirakian, A. & Kolin, A. Antimetastatic effect of amiloride in an animal
534 tumour model. *Anticancer Res* **8**, 1373-1376 (1988).
535
536 12. Evans, D. M. & Sloan Stakleff, K. D. Control of pulmonary metastases of rat
537 mammary cancer by inhibition of uPA and COX-2, singly and in combination. *Clin*
538 *Exp Metastasis* **21**, 339-346 (2004).
539
540 13. Hegde, M., Roscoe, J., Cala, P. & Gorin F. Amiloride kills malignant glioma cells
541 independent of its inhibition of the sodium-hydrogen exchanger. *J Pharmacol Exp*
542 *Ther* **310**, 67-74 (2004).
543

544 14. Leon, L. J., Pasupuleti, N., Gorin, F. & Carraway, K. L., 3rd. A cell-permeant
545 amiloride derivative induces caspase-independent, AIF-mediated programmed
546 necrotic death of breast cancer cells. *PLoS One* **8**: e63038
547 10.1371/journal.pone.0063038 (2013).
548
549 15. Pasupuleti, N., Leon, L., Carraway, K. L., 3rd & Gorin, F. 5-Benzylglycinyl-amiloride
550 kills proliferating and nonproliferating malignant glioma cells through caspase-
551 independent necroptosis mediated by apoptosis-inducing factor. *J Pharmacol Exp*
552 *Ther* **344**, 600-615 (2013).
553
554 16. Hu, M. & Carraway, K. L., 3rd. Repurposing cationic amphiphilic drugs and
555 derivatives to engage lysosomal cell death in cancer treatment. *Front Oncol* **10**,
556 605361 10.3389/fonc.2020.605361 (2020).
557
558 17. Rowson-Hodel, A. R. *et al*. Hexamethylene amiloride engages a novel reactive
559 oxygen species- and lysosome-dependent programmed necrotic mechanism to
560 selectively target breast cancer cells. *Cancer Lett* **375**, 62-72 (2016).
561
562 18. Berg, A. L. *et al*. The cationic amphiphilic drug hexamethylene amiloride eradicates
563 bulk breast cancer cells and therapy-resistant subpopulations with similar
564 efficiencies. *Cancers* **14**, 949 10.3390/cancers14040949 (2022).
565
566 19. Luo, J. & Tannock, I. F. Inhibition of the regulation of intracellular pH: potential of 5-
567 (N,N-hexamethylene) amiloride in tumour-selective therapy. *Br J Cancer* **70**, 617-
568 624 (1994).
569
570 20. Li, J. H., Cragoe, E. J. & Lindemann, B. Structure-activity relationship of amiloride
571 analogs as blockers of epithelial Na channels: I. Pyrazine-ring modifications. *J*
572 *Membr Biol* **83**, 45-56 (1985).
573
574 21. García-Cañero, R., Trilla, C., Pérez de Diego, J., Díaz-Gil, J. J. & Cobo, J. M.
575 Na+ :H+ exchange inhibition induces intracellular acidosis and differentially impairs
576 cell growth and viability of human and rat hepatocarcinoma cells. *Toxicol Lett* **106**,
577 215-228 (1999).
578
579 22. Aredia, F. *et al*. Multiple effects of the Na(+)/H (+) antiporter inhibitor HMA on cancer
580 cells. *Apoptosis* **18**, 1586-1598 (2013).
581
582 23. Harguindey, S., Arranz, J. L., Wahl, M. L., Orive, G. & Reshkin, S. J. Proton
583 transport inhibitors as potentially selective anticancer drugs. *Anticancer Res* **29**,
584 2127-2136 (2009).
585
586 24. Harguindey, S. *et al*. Cariporide and other new and powerful NHE1 inhibitors as
587 potentially selective anticancer drugs--an integral
588 molecular/biochemical/metabolic/clinical approach after one hundred years of cancer
589 research. *J Transl Med* **11**, 282 10.1186/1479-5876-11-282 (2013).
590

591 25. Amith, S. R., Wilkinson, J. M. & Fliegel, L. KR-33028, a potent inhibitor of the
592 Na(+)/H(+) exchanger NHE1, suppresses metastatic potential of triple-negative
593 breast cancer cells. *Biochem Pharmacol* **118**, 31-39 (2016).
594
595 26. Gorin, F. A., Pasupuleti, N., Mahajan, D. & Dugar, S. Killing glioma "stem-like" cells
596 via drug-induced relocation of endosomal urokinase proteins. *Anticancer Agents*
597 *Med Chem* **17**, 40-47 (2017).
598
599 27. Pasupuleti, N. *et al*. Intracellular urokinase uPA-PAI-1 complex: disruption by small
600 molecule targets hypoxically programmed glioma cells. *Open Access Journal of*
601 *Neurology & Neurosurgery* **7**, 18 10.19080/OAJNN.2018.07.555712 (2018).
602
603 28. Buckley, B. J. *et al*. 6-Substituted hexamethylene amiloride (HMA) derivatives as
604 potent and selective inhibitors of the human urokinase plasminogen activator for use
605 in cancer. *J Med Chem* **61**, 8299-8320 (2018).
606
607 29. Buckley, B. J. *et al*. Systematic evaluation of structure-property relationships and
608 pharmacokinetics in 6-(hetero)aryl-substituted matched pair analogs of amiloride
609 and 5-(N,N-hexamethylene)amiloride. *Bioorg Med Chem* **37**, 116116
610 10.1016/j.bmc.2021.116116 (2021).
611
612 30. Lee, Y. S., Sayeed, M. M. & Wurster, R. D. Intracellular Ca2+ mediates the
613 cytotoxicity induced by bepridil and benzamil in human brain tumor cells. *Cancer Lett*
614 **88**, 87-91 (1995).
615
616 31. Shono, Y. *et al*. Change in intracellular pH causes the toxic Ca2+ entry via NCX1 in
617 neuron- and glia-derived cells. *Cell Mol Neurobiol* **30**, 453-460 (2010).
618
619 32. Ross, D. D. *et al*. Atypical multidrug resistance: breast cancer resistance protein
620 messenger RNA expression in mitoxantrone-selected cell lines. *J Natl Cancer Inst*
621 **91**, 429-433 (1999).
622
623 33. Zhang, H. Y. *et al*. Effects of long noncoding RNA-ROR on tamoxifen resistance of
624 breast cancer cells by regulating microRNA-205. *Cancer Chemother Pharmacol* **79**,
625 327-337 (2017).
626
627 34. Lobo, S. Is there enough focus on lipophilicity in drug discovery? *Expert Opinion on Drug*
628 *Discovery* **15**, 261-263 (2020).
629
630 35. Showalter, M. R. *et al*. The emerging and diverse roles of bis(monoacylglycero)
631 phosphate lipids in cellular physiology and disease. *Int J Mol Sci* **21**, 8067
632 10.3390/ijms21218067 (2020).
633
634 36. Ellegaard, A. M., Bach, P. & Jäättelä, M. Targeting cancer lysosomes with good old cationic
635 amphiphilic drugs. *Rev Physiol Biochem Pharmacol* **185**, 107-152 (2023).
636

637 37. Boya, P. & Kroemer, G. Lysosomal membrane permeabilization in cell death.
638 *Oncogene* **27**, 6434-6451 (2008).
639
640 38. Hämälistö, S. & Jäättelä, M. Lysosomes in cancer-living on the edge (of the cell).
641 *Curr Opin Cell Biol* **39**, 69-76 (2016).
642
643 39. Serrano-Puebla, A. & Boya, P. Lysosomal membrane permeabilization as a cell
644 death mechanism in cancer cells. *Biochem Soc Trans* **46**, 207-215 (2018).
645
646 40. Berg, A. L. *et al*. Engaging the Lysosome and Lysosome-Dependent Cell Death in
647 Cancer in *Breast Cancer* (ed Mayrovitz, H. N.) Exon Publications, Brisbane AU,
648 2022.
649
650 41. Petersen, N. H. T. *et al*. Transformation-associated changes in sphingolipid metabolism
651 sensitize cells to lysosomal cell death induced by inhibitors of acid sphingomyelinase.
652 *Cancer Cell* **24**, 379-393 (2013).
653
654 42. Shibata, M. & Hoque, M. O. Targeting cancer stem cells: a strategy for effective
655 eradication of cancer. *Cancers (Basel)* **11**, 732 10.3390/cancers11050732 (2019).
656
657 43. Zhou, H. M., Zhang, J. G., Zhang, X. & Li, Q. Targeting cancer stem cells for
658 reversing therapy resistance: mechanism, signaling, and prospective agents. *Signal*
659 *Transduct Target Ther* **6**, 62 10.1038/s41392-020-00430-1 (2021).
660
661 44. Lyu, Y., Kopcho, S., Alvarez, F. A., Okeoma, B. C. & Okeoma C. M. Development of
662 a cationic amphiphilic helical peptidomimetic (B18L) as a novel anti-cancer drug
663 lead. *Cancers* **12**, 2448 10.3390/cancers12092448 (2020).
664
665 45. Li, X. *et al*. Bioengineered miR-27b-3p and miR-328-3p modulate drug metabolism and
666 disposition via the regulation of target ADME gene expression. *Acta Pharm Sin B* **9**, 639-
667 647 (2019).
668
669 46. Borowsky, A. D. *et al*. Syngeneic mouse mammary carcinoma cell lines: two closely
670 related cell lines with divergent metastatic behavior. *Clin Exp Metastasis* **22**, 47-59
671 (2005).
672
673 47. Miller, J. K. *et al*. Suppression of the negative regulator LRIG1 contributes to ErbB2
674 overexpression in breast cancer. *Cancer Res* **68**, 8286-8294 (2008).
675
676 48. Aina, O. H. *et al*. Canine malignant melanoma alpha-3 integrin binding peptides. *Vet*
677 *Immunol Immunopathol* **143**, 11-19 (2011).
678
679 49. Thomas, R. *et al*. Influence of genetic background on tumor karyotypes: Evidence
680 for breed-associated cytogenetic aberrations in canine appendicular osteosarcoma.
681 *Chromosome Res* **17**, 365-377 (2009).
682

683 50. Nytko, K.J., Thumser-Henner, P., Weyland, M. S., Scheidegger, S. & Rohrer Bley,
684 C. Cell line-specific efficacy of thermoradiotherapy in human and canine cancer cells
685 in vitro. *PLoS One* **14**, e0216744 10.1371/journal.pone.0216744 (2019).
686
687 51. Nguyen-Ngoc K. V. *et al*. ECM microenvironment regulates collective migration and local
688 dissemination in normal and malignant mammary epithelium. *Proc Natl Acad Sci USA* **109**,
689 2595-2604 (2012).
690
691 52. Rowson-Hodel, A. R. *et al*. Neoplastic transformation of porcine mammary epithelial
692 cells in vitro and tumor formation in vivo. *BMC Cancer* **15,** 562 10.1186/s12885-015-
693 1572-7 (2015).

694 **Acknowledgements**

695 We thank Dr. Frederic Gorin for providing compound 10357 and Dr. Aiming Yu for providing the
696 MX-100 MCF7 derivative cell line. This research was funded by NIH/NCI grants R01CA250211,
697 R01CA250211-S1, R01CA250211-S2, and R01CA230742-S1 (KLC). The UC Davis
698 Combinatorial Chemistry and Chemical Biology Shared Resource is supported by NIH/NCI
699 Cancer Center Support Grant P30CA093373 and was responsible for the synthesis and
700 purification of the compounds. A preprint version of this article may be found at bioRxiv:
701 https://www.biorxiv.org/content/10.1101/2023.05.25.542364v1.

702

703 **Author Contributions**

704 Participated in research design: Hu, Liu, Carraway

705 Conducted experiments: Hu, Liu, Castro, Huang, Loza-Sanchez, Learn

706 Contributed new reagents or analytic tools: Liu, Lam

707 Performed data analysis: Hu, Liu

708 Wrote or contributed to the writing of the manuscript: Hu, Carraway

709

710 **Data Availability Statement**

711 Data related to the synthesis and characterization of novel amiloride derivatives may be found in
712 the Supplementary Materials. Other primary data presented in this study are available on request
713 from the corresponding author.

714

715 **Competing Interests Statement**

716 The authors declare no conflicts of interest.